J. Fluid Mech. (1987), *vol.* 174, *pp.* 529–552
Printed in Great Britain

Timescale and structure of ejections and bursts in turbulent channel flows

By T. S. LUCHIK† AND W. G. TIEDERMAN
School of Mechanical Engineering, Purdue University, West Lafayette, IN 47907, USA

(Received 18 November 1985 and in revised form 9 June 1986)

Burst structures in the near wall region of turbulent flows are associated with a large portion of the turbulent momentum transport from the wall. However, quantitative measures of the timescales associated with the burst event are not well defined, largely due to ambiguities associated with the methods used to detect a burst.

In the present study, Eulerian burst-detection schemes were developed through extensions of the *uv* quadrant 2, VITA, and *u*-level techniques. Each of the basic techniques detects ejections. One or more ejections are contained in each burst and hence the key idea is to identify and to group those ejections from a single burst into a single-burst detection. When the ejection detections were grouped appropriately into burst detections, all of the extended techniques yielded the same average time between bursts as deduced from flow visualization for fully-developed channel flow in the range $8700 \leqslant Re_h \leqslant 17800$. The present results show that inner variables (wall shear stress and kinematic viscosity) are the best candidates for the proper scaling of the average time between bursts. Conditional velocity sampling during burst and ejection detections shows that these burst events are closely correlated with slower-than-average moving fluid, moving both away from the wall and toward the wall.

1. Introduction

The ejection of low-momentum fluid from the near wall region to the outer portion of the flow has been identified as a coherent structure associated with a large portion of turbulent kinetic energy and Reynolds stress production (Corino & Brodkey 1969; Kim, Kline & Reynolds 1971). These ejection structures contain fluid from low-speed streaks in the viscous sublayer.

A streak is a long narrow region of low-speed fluid very near the wall ($y^+ \leqslant 5$) (superscript + denotes that the quantity was made dimensionless using wall shear velocity, u_τ and kinematic viscosity, ν.). Streaks remain stable for some streamwise distance before they begin to oscillate and lift away from the wall. Finally, all or part of the streak filament ejects away from the wall in a coherent manner. This entire process is termed a burst. Within the burst, there may be one or more ejection structures (Offen & Kline 1985; Bogard & Tiederman 1986). Thus, a working definition of a burst is one or more ejections resulting from the same streak instability. The burst event occurs in a quasi-periodic manner and therefore experimentalists have concentrated their efforts on determining statistical quantities such as the average time between bursts and the average spanwise spacing of sublayer streaks.

† Present Address: Jet Propulsion Lab, California Institute of Technology, Pasadena, CA 91109, USA.

It is well known that for Newtonian flows the average streak spacing when normalized with inner variables, shear velocity and kinematic viscosity, has a non-dimensional value of about 100, independent of Reynolds number. However, there is no consensus about the scaling of the average time between bursts.

Flow visualization has been effective in giving a good qualitative description of the burst process. Even though the technique of Bogard & Tiederman (1983), gives an accurate estimate of the average time between bursts, it, like all other flow visualization techniques, is limited to rather low Reynolds numbers and does not readily yield statistical quantities based on conditional probabilities. Thus, several techniques for the detection of the Lagrangian burst event with velocity probes have been proposed and used. Most of these techniques require only the measurement of the streamwise component of velocity which is a desirable feature since multi component velocity measurements in the near wall region of a turbulent flow are difficult to obtain. The techniques are based on the principle that there is some recognizable pattern or level in the velocity signal associated with a burst event. However, the burst rate results obtained from the various techniques have conflicted among themselves and with those obtained from flow visualization. This occurred because each of the techniques has at least one adjustable parameter or threshold with no clear way to determine an appropriate value for it.

In an attempt to explain some of these differences, Bogard & Tiederman (1986) used simultaneous flow visualization and velocity-probe measurements to show that each of the more popular techniques were detecting ejection related phenomena. However, on a one-to-one basis none of the techniques were detecting all of the ejections, regardless of the value of the adjustable threshold. They did find that the 'best' correspondence, on a one-to-one basis, was obtained with the uv quadrant 2 technique of Lu & Willmarth (1973). Using this technique with a second filtering parameter, the maximum time between ejections from the same burst, they were able to group probe 'ejection' detections into probe 'burst' detections. Furthermore, there was a range of the adjustable threshold over which the number of probe burst detections remained constant and was equal to the number detected by flow visualization. However, as the name implies, the uv quadrant 2 technique requires accurate two-component velocity measurements. Bogard & Tiederman did not attempt to use any of the single component techniques with the grouping technique. One objective of the present study is to build on the ideas of Bogard & Tiederman (1986) and to develop additional velocity-probe burst detection techniques.

Recently, several authors (Blackwelder & Haritonidis 1983; Willmarth & Sharma 1984; Alfredsson & Johansson 1984) have used the variable interval time average (VITA) technique of Blackwelder & Kaplan (1976) with a positive gradient condition at the centre of detection to study the scaling of the turbulent wall-layer structure. However, the results of these studies have been somewhat conflicting. While Blackwelder & Haritonidis (1983) and Willmarth & Sharma (1984) have shown that the burst rate scales with inner variables, Alfredsson & Johansson have used a mixed timescale to scale the wall-layer structure. The second objective of the present study was to give additional data for evaluating the appropriate timescaling of the burst event.

Finally, conditional statistics based on the detection of burst and ejection structures for the streamwise fluctuating velocity u, the fluctuating velocity component normal to the wall, v and the uv product are presented. These statistics are used to determine which technique yields an accurate estimate of the burst and

ejection process by direct comparison to the conditional statistics presented by Bogard (1982) who used flow visualization to detect these structures.

2. Experimental considerations

2.1. *Flow loop*

The experiments were performed in a recirculating flow loop with a rectangular cross-section channel as the test section. Provisions were made in an upstream stilling tank such that the fluid entered the test section without any large-scale vorticity (Tiederman, Luchik & Bogard 1985). At the downstream end of the flow channel, a large stilling tank provided damping of disturbances created from the outlet. Located in this stilling tank was a cooling coil that maintained the water temperature in the channel at 24 °C during an experiment.

The two-dimensional flow channel had an internal cross-section of 2.5×25.0 cm. Located in the bottom plate of the test section were a thin (0.127 mm wide) slot used for flow visualization and a series of pressure taps, which were used to monitor the pressure gradient throughout an experiment. Velocity measurements were made in the centre third of the channel span, more than 125 channel heights downstream of the inlet and more than 70 channel heights upstream of the outlet. These measurements were made at $y^+ = 30$ for a range of Reynolds numbers, $9400 \leqslant Re_h \leqslant 17800$. The Reynolds number is based on mass averaged velocity and the channel height of 2.5 cm.

Two micrometre manometers with carbon tetrachloride as the manometer fluid were used to measure the pressure gradient in the test section. With this manometer fluid, pressure-drop measurements could be made with a sensitivity of 0.015 mm of water. Additional details of the experimental apparatus appear in Luchik (1985).

2.2. *Velocity measurements*

Simultaneous measurements of the streamwise velocity component, U, and the normal velocity component, V, were made using a forward scatter version of a Thermo-Systems Incorporated (TSI) model 9100-8 three-beam, two-colour laser velocimeter. The system included frequency shifting at 40 MHz with electronic down mixing, 2.27 beam expansion, and dual aperture collection to minimize optical noise and to allow finer focusing on the probe volume.

The photomultiplier tubes outputs were processed using TSI model 1980 counter type processors. Each processor was operated in the N-cycle mode with $N = 8$. Only one data point was taken per Doppler burst. A coincidence window was used to ensure that the measurements of U and V were obtained from the same particle.

The data collection electronics included a Digital Equipment Corporation PDP 11/03 minicomputer and TSI model 1998 interfaces. Data were stored temporarily on floppy disk prior to being transferred to a VAX 11/780 for initial data reduction. Data were then transferred to CDC 6500 and 6600 computers for further analysis and permanent storage.

The two-component data were taken at angles of $\pm 45°$ to the main flow direction so that the three-beam system could be traversed as close to the wall as possible. Velocities at these angles were calculated using

$$U_{\mathrm{i}|+45} = f_{\mathrm{R}|+45}\,(f_{\mathrm{Di}|+45} - f_{\mathrm{s}|+45}), \tag{1}$$

and

$$U_{\mathrm{i}|-45} = -f_{\mathrm{R}|-45}\,(f_{\mathrm{Di}|-45} - f_{\mathrm{s}|-45}). \tag{2}$$

	Blue	Green
Probe volume length (mm)	1.024	1.080
Probe volume diameter (μm)	52.4	55.2
Fringe spacing (μm)	3.402	3.624
Effective frequency shift (MHz)	−1.0	+1.0
Beam spacing (mm)	35.3	35.3

TABLE 1. Two-component laser velocimeter parameters

Here f_R is the fringe spacing, f_{Di} is the Doppler frequency, f_s is the effective frequency shift after electronic downmixing, U_i is the measured velocity component and the subscripts ± 45 are the angles in degrees with respect to the streamwise direction at which the measurements were made. Note the sign difference is due to the fact that positive frequency shifting had to be used on one colour of the velocimeter. These direct measurements were decomposed into streamwise and normal velocity components using a standard rotation of axes such that

$$U_i = 0.7071\,(U_{i|+45} + U_{i|-45}), \tag{3}$$

$$V_i = 0.7071\,(U_{i|+45} - U_{i|-45}), \tag{4}$$

where U_i is the instantaneous streamwise velocity component and V_i is the instantaneous velocity component normal to the wall. This arrangement of beams does have the advantage of allowing measurements close to a wall. However, the disadvantage is that the normal component of velocity is calculated from the difference between two numbers of nearly the same magnitude. The LDV parameters used in the present study are listed in table 1.

The velocity data that were used in probe detection algorithms were taken as fast as possible. Typically the data rate was greater than 2000 Hz. The time between adjacent data points was recorded also. These data were used to reconstruct the real-time velocity signal which was sampled at a rate equal to the viscous timescale, u_τ^2/ν. Because of the data storage limitation of the PDP minicomputer, multiple data records were taken in this fashion so that the total velocity record was longer than 400 average burst periods.

3. Probe detection algorithm

Velocity-probe techniques for the detection of the Lagrangian burst event have been devised because flow visualization yields limited quantitative information about the burst event and is limited to relatively low Reynolds numbers. In the present study, three basic probe techniques were examined; the *uv* quadrant 2, the variable interval time average (VITA) and the *u*-level techniques. In the following sections, the techniques will be discussed and evaluated on a one-to-one basis as well as an average basis. The one-to-one evaluation uses the simultaneous flow visualization and hot-film data at $y^+ = 15$ of Bogard (1982). These simultaneous measurements were made at a Reynolds number of 8700 based on mass average velocity in a channel with a height of 6.0 cm.

3.1. *Description of the probe detection techniques*

The uv quadrant 2 technique has a broader physical base than the other techniques used in this study. Since an ejection is defined as low-momentum fluid that is lifting away from the wall, it follows that when an ejection passes through the detection point there will be an instantaneous defect from the mean in the streamwise component of velocity and a positive normal component of velocity, thus a quadrant 2 uv event in the velocity fluctuation coordinates (u, v).

The quadrant 2 technique is a simple level detector because an ejection event is said to have occurred when the instantaneous uv product is in the second quadrant and is greater in magnitude than the product of the r.m.s. streamwise and normal velocities and a threshold, H, or

$$|uv|_2 \geqslant Hu'v', \tag{5}$$

where the superscript prime denotes an r.m.s. value. One major advantage of this technique is that it detects the physical situation associated with an ejection, however it does require accurate measurements of both U and V near a wall. Measurement of V increases the experimental difficulty and cost considerably.

The VITA technique introduced by Blackwelder & Kaplan (1976) is the most widely used probe technique for detecting bursts. The basic idea is that when an ejection passes through the detection point, there will be a rapid change in the instantaneous streamwise velocity component. This rapid change will produce a high level of the variance of the streamwise velocity which is detected by the technique. However, Johansson & Alfredsson (1982) noted that a high level of variance was associated with both acceleration and decelerations. They identified the acceleration as the event of interest because it was associated with high levels of uv. The technique in its functional form is given by

$$\mathrm{VAR} = \tilde{U}^2 - \tilde{U}^2, \tag{6}$$

where

$$\tilde{U} = \frac{1}{T_A} \int_{t-\frac{1}{2}T_A}^{t+\frac{1}{2}T_A} U \, \mathrm{d}t. \tag{7}$$

An event is detected when

$$\mathrm{VAR} > ku'^2, \tag{8}$$

and validated as an ejection-related event when

$$\frac{\mathrm{d}U}{\mathrm{d}t} > 0, \tag{9}$$

at the centre of detection. Here k is a threshold level, u'^2 is the long-time variance and T_A is a relatively short time chosen to filter the velocity signal. One advantage of this technique is that only the streamwise component of velocity is required for its implementation. However, the major disadvantage of the technique is that two adjustable parameters, k and T_A, must be fixed.

The u-level technique of Lu & Willmarth (1973) is the least commonly used technique of those studied here. The implementation of the technique is quite simple and the amount of data required for its use is minimal. This probe technique merely looks for deficits from the mean streamwise velocity component and identifies an event when

$$u < -Lu', \tag{10}$$

where L is a threshold level. An interesting point is that for strongly negative correlated uv data, as is found near a wall, this technique should detect nearly the same number of events as the uv quadrant 2 technique. Because of this similarity, the ease of use of the u-level technique and the findings of Bogard (1982), that both quadrant 2 and quadrant 3 uv are associated with the ejection event, this technique was investigated with more vigour than in the past.

3.2. *Analysis of techniques*

The evaluation of these techniques on a one-to-one basis requires the definition of two new variables (Bogard 1982). They are

$$P(\mathrm{E}) = \frac{N_{\mathrm{ED}}}{N_{\mathrm{E}}}, \tag{11}$$

and

$$P(\mathrm{D}) = \frac{N_{\mathrm{DV}}}{N_{\mathrm{D}}}, \tag{12}$$

where N_{E} is the total number of visually marked events, N_{D} is the total number of probe detections, N_{ED} is the number of visually marked events that correspond to probe detected events and N_{DV} is the number of probe detections that corresponds to a visually marked event. An additional factor for this evaluation is the comparison of $P(\mathrm{E})$ and $P(\mathrm{D})$ when the total number of probe detections, N_{D}, is equal to the total number of visually marked events, N_{E}. The number of visually marked ejection events was 164 and the corresponding probabilities are indicated by an arrow in figures 1 and 2.

Figure 1 shows the probability profiles for the quadrant 2, VITA and u-level techniques. At very low threshold levels, all of the probe techniques except VITA detected nearly all of the visually marked events, and $P(\mathrm{E})$ approaches 1; however, there were also a large number of probe detections which did not correspond to a visual ejection and $P(\mathrm{D})$ is low. At high threshold levels, nearly all of the probe detections corresponded to a visual ejection and $P(\mathrm{D}) = 1$; however, a large percentage of the visual events were not detected. It is important to note that when $P(\mathrm{E}) < P(\mathrm{D})$ at $N_{\mathrm{D}} = 164$, the probe detection techniques are yielding multiple detections per visual ejection. In the ideal case, the probe technique would detect each ejection only once while detecting all of the ejections.

For the VITA technique, the averaging time, T_{A}, was fixed using $U_0 T_{\mathrm{A}}/a = 0.9$ where U_0 is the centreline velocity and a is the channel half-height. For this averaging time the number of detections was maximized independent of threshold. A similar result was noted by Johansson & Alfredsson (1982). It is also worth noting that at any level of threshold, the VITA technique yields a much lower probability of detecting an ejection, $P(\mathrm{E})$, than the other two methods.

Because the quadrant 2 and u-level techniques were yielding multiple probe detections per visual ejection when $N_{\mathrm{D}} = N_{\mathrm{E}}$, it was desirable to modify both of these techniques such that each technique would yield one probe detection per visual ejection. The modification was to turn the detector function on at one level and turn it off at a second lower level. Two thresholds were used by Robinson (1982) for a quite different purpose. He used two thresholds with the VITA technique to identify events with magnitudes between the two thresholds. Here the concept is to leave the detector 'on' and eliminate multiple detections of a single event that are caused by relatively small amplitude fluctuations in the signal. This concept produced no improvement for the quadrant 2 technique due to the rather large, highly intermittent excursions in the uv signal.

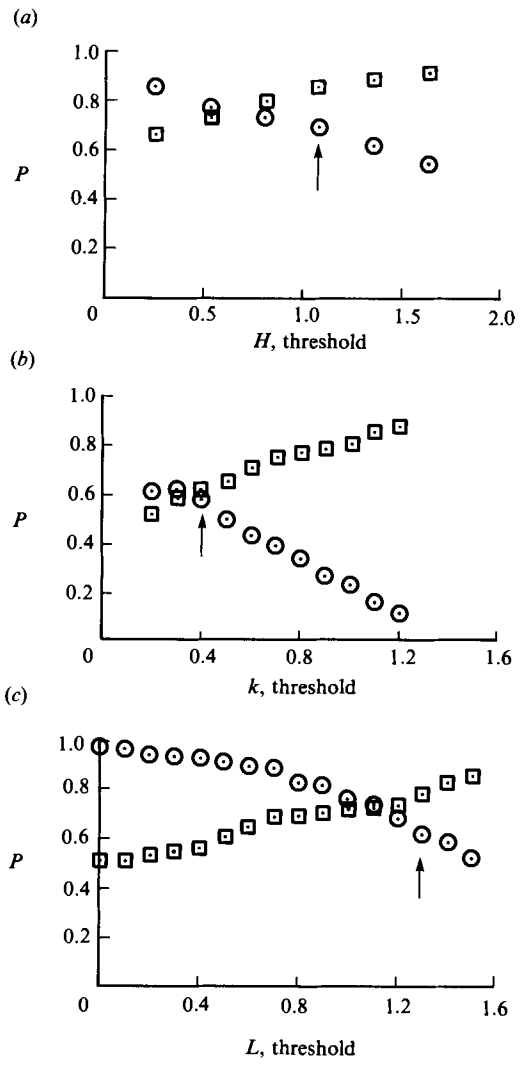

FIGURE 1. Probability variation with threshold for (*a*) *uv* quadrant 2, (*b*) VITA, (*c*) *u*-level techniques. □, *P*(D); ○, *P*(E).

The *u*-level technique did yield better results when modified. 'Off' threshold levels ranging from 0 to 1.0 *L* were investigated. The best results were found when the detector function was turned on when

$$u < -Lu', \tag{13}$$

and turned off when

$$u \geqslant -0.25\, Lu'. \tag{14}$$

This technique will be referred to as the modified *u*-level or *mu*-level technique throughout the rest of the text.

Figure 2 shows the probability profiles for this technique. As can be seen by comparing figure 1 and 2, there is a substantial improvement in the probability of detecting an ejection, *P*(E), while *P*(D) only decreased slightly when $N_D = 164$, indicated by the arrow on the figure. Since *P*(E) = *P*(D) at this location, the technique

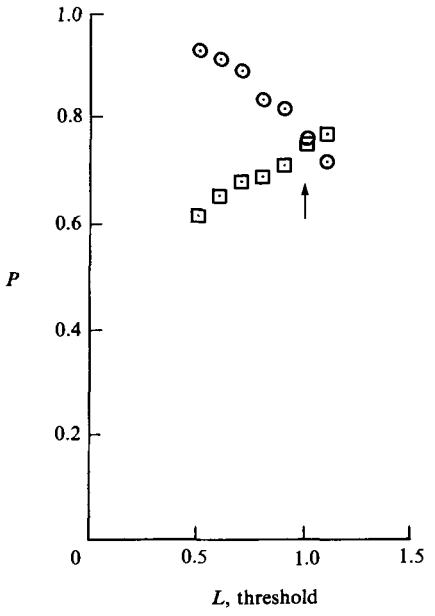

FIGURE 2. Probability variation with threshold for the modified u-level technique. □, P(D); ○, P(E).

Technique	Threshold	N_{ED}	P(E)	N_D	N_{DV}	P(D)
$uv\|_2$	1.209	106	0.646	163	140	0.859
VITA	0.4	95	0.579	166	102	0.613
u-level	1.28	104	0.634	163	126	0.773
mu-level	1.00	124	0.756	166	124	0.747

TABLE 2. Results for all techniques with $N_D \approx 164$

is yielding one probe detection per visual ejection. The probability results for all of the techniques are summarized in table 2 for the situation when $N_D = 164 \pm 2$.

As noted by Bogard & Tiederman (1986) the probe techniques studied here are ejection detectors. Further inspection of the velocity records reveals that the two level detectors are detecting the leading edge of the ejection while the VITA technique detects the trailing edge. Since each of the techniques detects some sub-event of the burst, which is the event of interest, any of these techniques may be useful burst detectors.

3.3. *Methods for deducing time between bursts*

The method for separating or grouping ejection detections into burst detections is a filtering technique originated by Bogard & Tiederman (1986). A new parameter, τ_E, the maximum time between ejections from the same burst is defined. The appropriate value of this new parameter can be determined using various methods based on the concept that ejections may be grouped into two temporal distributions; one for ejections from the same burst and one for ejections from different bursts. Ideally, the combined distribution would be like the one shown in figure 3, where there is a clear distinction between the two types of events. However, the actual

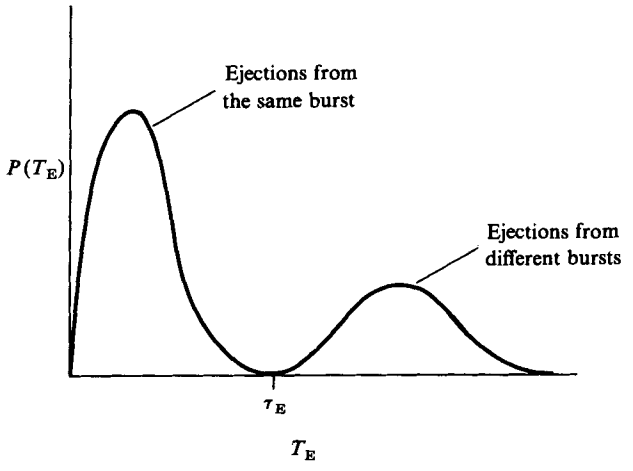

FIGURE 3. Schematic showing idealized probability distribution of time between ejections.

distributions overlap enough such that usually there is no clear break in the distribution for all ejections. Therefore, techniques were developed to obtain an appropriate deterministic method for obtaining a value of the grouping parameter such that the two distributions are separated properly.

In the following sections, methods of separating ejection detections into burst detections for the four probe detection techniques are presented. These methods of separation were developed at $y^+ = 15$ and $Re_h = 8700$ and verified at $y^+ = 30$ and $Re_h = 8700$ (see Luchik 1985) prior to application at higher Reynolds numbers. The results presented are for $y^+ = 30$ and $Re_h = 17800$.

3.3.1. *Quadrant 2 and u-level techniques*

The quadrant 2 and u-level techniques both yielded multiple probe detections per visual detection. This skewed the distribution of the time between ejections (T_E) toward zero which resulted in this distribution resembling an exponential distribution. Because of this, a slight variation on the technique of Bogard & Tiederman (1986) was used to group probe ejection detections into probe burst detections.

When the cumulative probability of $T > T_E$ as a function of T_E was plotted in semi-log coordinates for a given threshold level, three straight lines emerged. A typical example for the quadrant 2 technique with $H = 1.0$ and $Re_h = 17800$ is shown in figure 4. Similar results were obtained for the u-level technique. From this graph, two distributions are clearly present, one for $T_E \leqslant 0.01$ s (region 1) and one for $T_E \geqslant 0.04$ s (region 2). The middle straight line, referred to as the overlap region, is some combination of the other two. The appropriate value for τ_E exists within the overlap region; however, as can be seen from figure 4, this region is rather large. The method for choosing the value of τ_E was to use the value of T_E at the intersection of a line extrapolated from region 1 and a line extrapolated from region 2, indicated by the arrow on figure 4.

The data in figure 4 are for $H = 1.0$ which is an appropriate first estimate of the correct threshold for the quadrant 2 technique. The first estimate threshold for the u-level technique was $L = 1.0$. These choices were based on the probability profiles shown in figure 1. Once an appropriate value for the grouping parameter, τ_E, is obtained, its incorporation into the basic probe detection technique is quite simple.

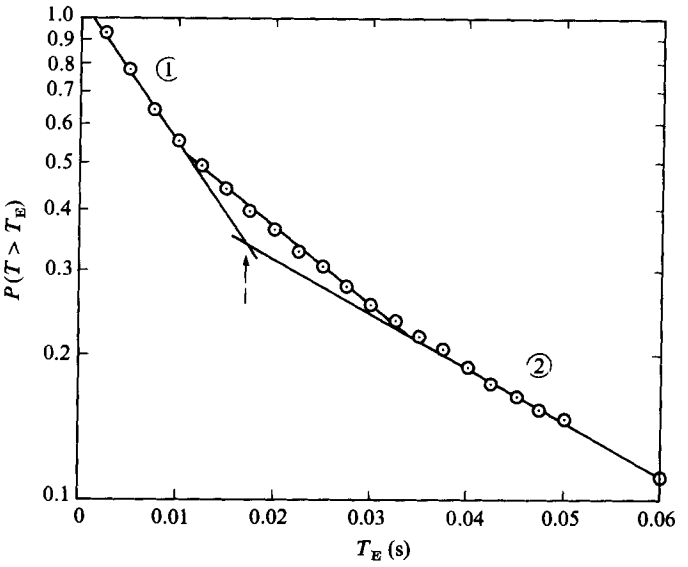

FIGURE 4. Cumulative probability distribution of time between ejections using the uv quadrant 2 technique with $H = 1.0$.

By knowing the time between adjacent ejections and comparing this time to the value of τ_E, one can determine whether any two ejections adjacent in time are from the same burst or from different bursts. By incorporating the grouping procedure into the basic probe detection algorithm, a region of threshold level over which the number of burst detections remain constant or have a slight minimum will result. This region of threshold independence should include the threshold level used to determine the value of τ_E. If this does not occur, the level of threshold should be iterated until the threshold independent range includes the threshold used to determine τ_E.

The variation in the average time between bursts with threshold at $Re_h = 17\,800$ and $y^+ = 30$ for the quadrant 2 technique is shown in figure 5. From this figure it is clear that there is good agreement between the flow-visualization data of Luchik & Tiederman (1984) and the present probe data. The grouping parameter varied less than $\pm 10\,\%$ for threshold levels $0.25 \leqslant H \leqslant 1.25$ for the quadrant 2 technique which resulted in approximately a $7\,\%$ variation in the number of burst detections.

Similar results were obtained using the u-level technique. However, agreement with flow visualization was not quite as good for this technique. Also, τ_E varied about $\pm 15\,\%$ for $0.25 \leqslant L \leqslant 1.25$ which changed the average time between bursts about the same amount. For both the quadrant 2 and the u-level technique the uncertainty of the results was significant when data records shorter than 200 burst periods were used. The present results were obtained using data records longer than 400 burst periods.

3.3.2. *Modified u-level and VITA techniques*

Examination of the data of Bogard & Tiederman (1986) for flow-visualization marked events reveals that the distribution of ejections from the same burst resembles a Poisson distribution. Further examination of these data show that quantitative agreement between the experimental data and the Poisson distribution

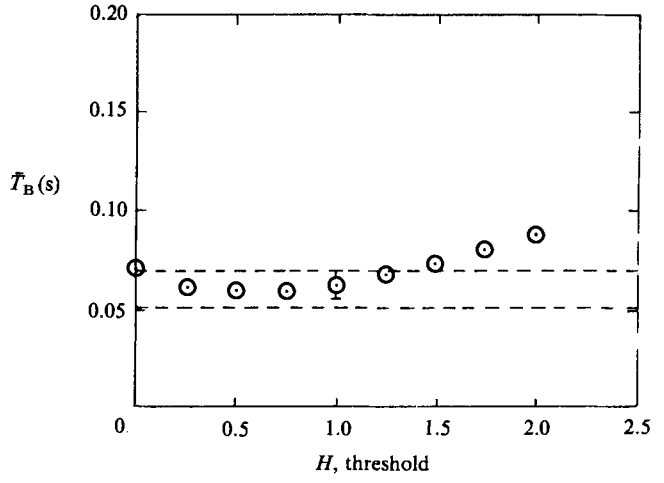

FIGURE 5. Variation in the average time between bursts using the uv quadrant 2 technique with T_E determined using the exponential distributions and $H = 1.0$, $\tau_E = 0.018$ s. I, 95 % confidence interval; = = =, 95 % confidence interval of flow visualization data from Luchik & Tiederman (1984).

is good. The Poisson distribution predicts that 95 % of the ejections from the same burst will occur for $T_E \leqslant 0.9$ s while 95 % of the experimental data occurs for $T_E \leqslant 0.8$ s.

Since the modified u-level technique was in good agreement on a one-to-one basis with flow visualization and also gave a reasonable estimate of the average duration of an ejection at a point in the flow, it was hypothesized that the mu-level technique would yield a distribution of time between ejections similar to the one obtained from flow visualization. Since the modified u-level and VITA ejection detections were distributed similarly, a Poisson distribution method for estimating τ_E was used for both techniques.

Implementation of the Poisson distribution separation technique is quite simple. The mode of the experimental distribution is set equal to the mean value of a hypothesized Poisson distribution. τ_E is then chosen as the value of T_E where $P(T \leqslant T_E) = 0.95$ for the Poisson distribution. As a starting point for the mu-level technique, the threshold level was chosen equal to unity since the probability profile for this technique (figure 2) indicated good correspondence with flow visualization at this level. The initial threshold level for the VITA technique was chosen to be that threshold where $P(\mathrm{E}) = P(\mathrm{D})$, which was $k = 0.3$–0.4 in the present study. The same criterion for determining the correct combination of grouping parameter and threshold level was used for the mu-level and VITA techniques as for the $uv|_2$ and u-level techniques. Use of the value of τ_E with the mu-level and VITA techniques to group ejections into bursts is identical to that for the quadrant 2 and u-level techniques. The grouping parameter varied less than 10 % for $0.5 \leqslant L \leqslant 1.25$ for the modified u-level technique which resulted in approximately ± 10 % variation in $\overline{T}_B$. For the VITA technique the variation in the grouping with threshold level for $0.2 \leqslant k \leqslant 0.4$ was 10 % which also resulted in an uncertainty of ± 10 % in $\overline{T}_B$ over the same range of threshold. When using the Poisson separation technique, it is important to note that the resolution of the grouping parameter is a function of the bin width used in the histograms. Finally, it should be noted that the VITA technique

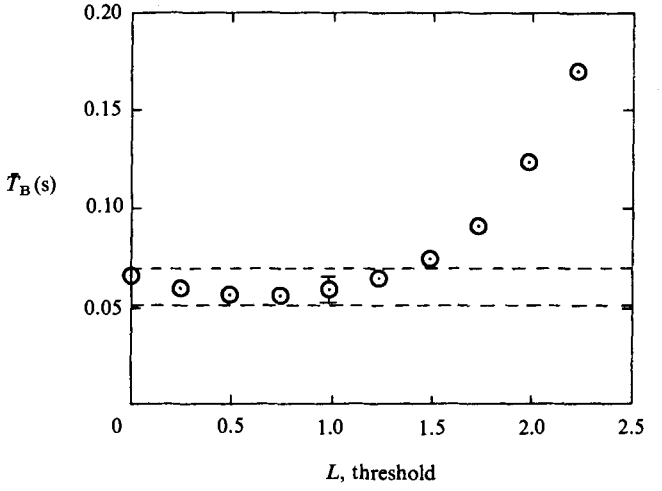

FIGURE 6. Variation in the average time between bursts for the *mu*-level technique with τ_E determined using the Poisson method, and $L = 1.0$, $\tau_E = 0.02$ s. I, 95% confidence interval; = = =, 95% confidence interval of flow-visualization data from Luchik & Tiederman (1984).

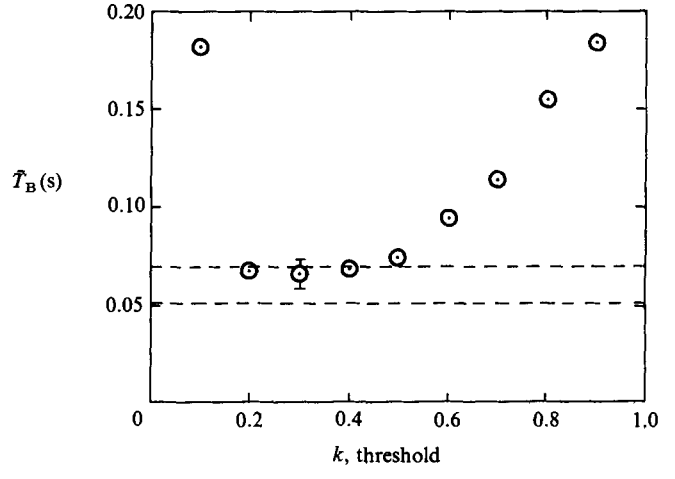

FIGURE 7. Variation in the average time between bursts for the VITA technique with τ_E determined using the Poisson method and $k = 0.4$, $\tau_E = 0.022$ s. I, 95% confidence interval; = = =, 95% confidence interval of flow-visualization data from Luchik & Tiederman (1984).

yielded consistent results with data records as short as 80 burst periods. This was a substantially shorter record than those required by the other techniques.

The results in terms of average time between bursts for the modified *u*-level and VITA techniques are presented in figures 6 and 7.

3.3.3. *Summary of detection algorithms*

Each of the techniques discussed exhibit good correspondence with flow visualization in terms of determining an average time between bursts. However, some of the techniques are more accurate than others. The $uv|_2$ technique is the best of the techniques used in the present study when large data sets are available (more than 200 bursting periods). It yields the smallest amount of error associated with the

grouping parameter and thus the smallest uncertainty in the value of the average time between bursts. The modified u-level and VITA technique were tied for second. Each of these techniques has the advantage of requiring only single-component data. Moreover, the VITA technique with T_A set such that the maximum number of detections are obtained for any threshold, yields a more consistent value for $\overline{T}_B$ when smaller data sets are used. The shortcoming of the VITA technique is the small range of threshold independence. For the VITA technique this range changed from $0.1 \leqslant k \leqslant 0.6$ at $Re_h = 8700$ to $0.2 \leqslant k \leqslant 0.5$ at $Re_h = 17800$. This trend is clearly not favourable. Studies at higher Reynolds numbers are needed to verify this trend over a larger range of Reynolds numbers.

In cases where larger data sets are available, the modified u-level technique is quite desirable. This technique exhibits no flat region although the rate of change in T_B over the range $0.25 \leqslant L \leqslant 1.25$ was small. The accuracy of these data were nearly the same as the $uv|_2$ technique. However, the existence of a threshold-independent region makes the $uv|_2$ technique more desirable.

Finally, the u-level technique, although it showed good agreement with the visual data at $Re_h = 17800$, had the largest amount of uncertainty associated with the proper value of the grouping parameter and the largest uncertainty in the estimate of the average time between bursts.

3.4. *Average time between bursts for channel flows of water*

Part of the rationale for developing a probe burst detection algorithm was to determine how the average time between bursts scales at high Reynolds numbers where flow visualization is impractical. Figure 8 shows the variation in the average time between bursts determined using the various probe techniques, with Reynolds number scaled with outer variables. Flow visualization data are also shown on this plot. It is clear that each of the probe techniques yields results which are in good agreement with the flow visualization results. Figures 9 and 10 show representative values of the average time between bursts normalized with inner variables and the mixed timescale recommended by Alfredsson & Johansson (1984) as a function of Reynolds number. The results presented in figures 8, 9 and 10 show similar trends for all three methods for normalizing the average time between bursts. For $Re_h < 10000$ dimensionless times increase because the favourable pressure gradient in the channel is substantial. For $Re_h > 10000$, the pressure gradient is no longer a factor and all three normalizations appear to approach constant values. For outer scaling,

$$T_{BO} = \frac{U_0}{\frac{1}{2}h}\overline{T}_B \approx 4, \tag{15}$$

for inner scaling,

$$T_B^+ = \frac{u_\tau^2}{\nu}\overline{T}_B \approx 90, \tag{16}$$

and for mixed scaling,

$$T_{BM} = \frac{\overline{T}_B}{\left|\frac{\nu}{u_\tau^2}\frac{\frac{1}{2}h}{U_0}\right|^{\frac{1}{2}}} \approx 20. \tag{17}$$

However, since the flow field is fully developed, there is a unique relationship between shear velocity and the Reynolds number as well as a unique relationship between the ratio of centreline velocity to bulk average velocity, U_m, and Reynolds number. As a result, at most only one of the three trends given by (15)–(17) can be correct. For example, if (15) is correct, then correlations for u_τ and U_0/U_m for fully developed channel flows can be used to renormalize $\overline{T}_B$ with either inner or mixed variables. The results from this type of argument yield a rather sensitive test of (15), (16) and (17).

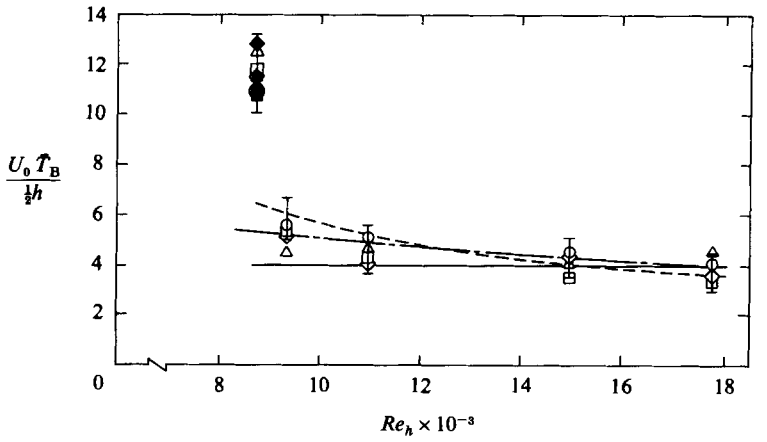

FIGURE 8. Effect of Reynolds number on the average time between bursts normalized with outer variables for the various probe detection algorithms with the appropriate value of τ_E. ◇, uv quadrant 2; △, u-level; □, modified u-level; ○, VITA; I, 95% confidence interval of flow visualization data; closed symbols, $y^+ = 15$; open symbols, $y^+ = 30$; $T_{BO} = 4$; – – –, $T_B^+ = 90$; — · —, $T_{BM} = 20$.

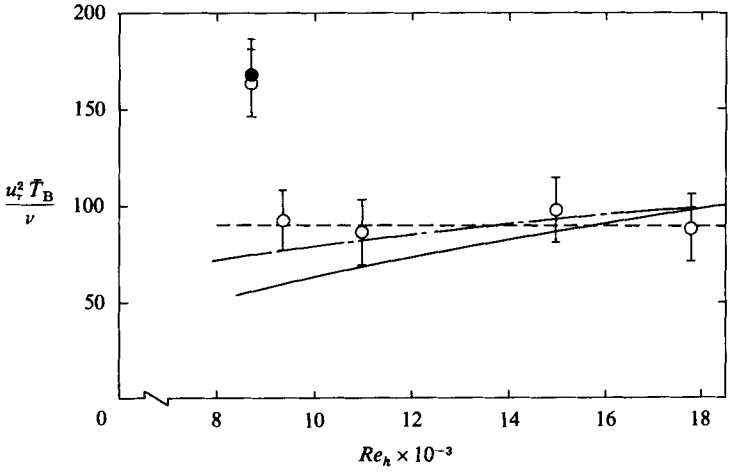

FIGURE 9. Effect of Reynolds number on the average time between bursts scaled with inner variables, representative values; shaded symbols, $y^+ = 15$; open symbols, $y^+ = 30$; ——, $T_{BO} = 4$; – – –, $T_B^+ = 90$; — · —, $T_{BM} = 20$.

In the following paragraphs, one of equations (15)–(17) will be assumed to be correct and the implications of that assumption will be investigated. The relevant correlations for fully developed smooth channels recommended by Dean (1978) are

$$u_\tau^2 = 0.073 \tfrac{1}{2} U_m^2 Re_h^{-\frac{1}{4}}, \tag{18}$$

and

$$\frac{U_0}{U_m} = 1.28 Re_h^{-0.0116}. \tag{19}$$

If (15) is correct, then (18) and (19) may be used to renormalize $\bar{T}_B$ in (15). The results are

$$\frac{u_\tau^2 \bar{T}_B}{\nu} = 0.057 Re_h^{0.762}, \tag{20}$$

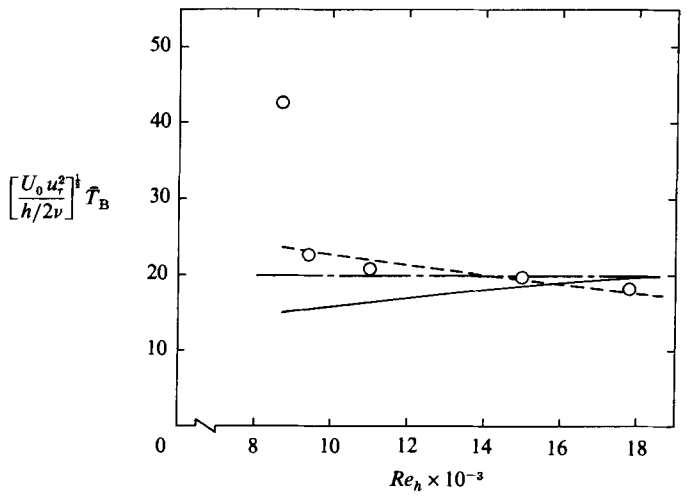

FIGURE 10. Non-dimensional burst period normalized with a mixed timescale as a function of Reynolds number; typical data from $y^+ = 30$. ——, $T_{BO} = 4$; – – –, $T_B^+ = 90$; — · —, $T_{BM} = 20$.

and
$$\left|\frac{U_0 u_\tau^2}{h/2\nu}\right|^{\frac{1}{2}} \bar{T}_B = 0.479\, Re_h^{0.381}. \tag{21}$$

The trends estimated by (20) and (21) are shown by the solid lines on figures 9 and 10. Clearly (20) and (21) do not agree with the data.

If (17) is correct, then similar use of (18) and (19) yields

$$\frac{U_0 \bar{T}_B}{\frac{1}{2}h} = 167.5\, Re_h^{-0.381}, \tag{22}$$

and
$$\frac{u_\tau^2 \bar{T}_B}{\nu} = 2.39\, Re_h^{0.381}. \tag{23}$$

Equations (22) and (23) are shown as the long–short–long dashed lines on figures 8 and 9. The agreement with the data in figure 8 is good but the assumption does not predict the trend shown by the data in figure 9.

Finally, if (16) is correct, then (20) and (21) may be used to give

$$\frac{U_0 \bar{T}_B}{\frac{1}{2}h} = 6313\, Re_h^{-0.762}, \tag{24}$$

and
$$\left|\frac{U_0 u_\tau^2}{\frac{1}{2}h\,\nu}\right|^{\frac{1}{2}} \bar{T}_B = 754\, Re_h^{-0.381}. \tag{25}$$

This assumption that inner scaling is correct is compared to the data in figures 8 and 10 (see dotted lines). In both cases, the predictions agree well with the experimental data.

Obviously, the best test of the scaling procedures will occur when reliable results are obtained at higher Reynolds number. The present range includes the maximum Reynolds number attainable in our flow facility with current pumps. Nonetheless, the present data, as tested in preceding paragraphs, indicates that outer scaling is not correct and that inner scaling is more appropriate than mixed scaling.

4. Conditionally sampled velocity characteristics

In the previous section, each of the probe detection techniques was shown to give a reasonable estimate of the average time between bursts when used with an appropriate value of the grouping parameter, τ_E. However, when obtaining conditional velocity averages, it is not only important for the probe technique to have a high probability of detecting an ejection, but it is equally important that the technique detect the entire event. Otherwise the technique will yield conditional velocity signatures which are not characteristic of the visual event. Therefore each of the four probe techniques was evaluated further using the data of Bogard (1982) at $Re_h = 8700$ and $y^+ = 15$ and the conditionally averaged quantities deduced by Bogard (1982) when flow visualization was the detector of ejections.

For this evaluation the thresholds of the probe techniques were chosen such that the number of probe detections was approximately equal to the number of visual ejections, the thresholds at which probe techniques yielded the correct value for the average time between ejections. High thresholds, where the probability of a valid detection is high but the probability of detecting an ejection is low, were not used because at these thresholds only the stronger events are detected and this would yield unrealistically high conditional averages. Low thresholds, where nearly all ejections are detected with a large number of invalid probe detections, were not used because the invalid detections would scramble with the valid detections resulting in unrealistically low conditional averages. The parameters chosen for comparison were: (i) the average duration of the event which is given by

$$\bar{T}_D = \frac{1}{N_D} \Sigma T_{Di}, \tag{26}$$

where T_{Di} is the duration of a probe detected event; (ii) the percentage contribution of uv in a given quadrant during all ejections compared to the total uv in that quadrant which is given by

$$100 \times \frac{\Sigma (uv_D)_i}{\Sigma (uv)_i}, \tag{27}$$

where $(uv_D)_i$ is the uv in quadrant i during a detection and $\Sigma(uv)_i$ is the total uv in quadrant i; (iii) the percentage contribution to the time average uv from each quadrant during an ejection given by

$$100 \times \frac{\Sigma (uv_D)_i}{\Sigma (uv)}, \tag{28}$$

and (iv) the ensemble average of the streamwise fluctuating velocity, the ensemble average of the normal fluctuating velocity and the ensemble average of the turbulent shear stress during an ejection.

A comparison of the conditionally sampled quantities obtained using the four probe detection techniques with the conditional samples based on flow visualization of Bogard (1982) is given in table 3. From this table it is clear that the modified u-level technique yields the best estimate of the values obtained using flow visualization as the detector. By having an 'off' level lower than the 'on' level, the modified u-level technique is much better at capturing most of the visual detections as shown by the good correspondence in the duration of the events. There is also good correspondence in the amount of uv measured with modified u-level and visual detection of the events. It is also worth noting that the uv_2 technique detects that portion of the ejection event associated with the occurrence of a high level of quadrant 2 uv; however, the duration

		Visual	*mu* level	*u* level	uv_2	VITA
Number of detections		163	163	163	161	162
$\bar{T}_E$ (s)		1.23	1.23	1.23	1.24	1.23
$\bar{T}_{DE}$ (s)		0.386	0.286	0.161	0.091	0.120
Intermittency		0.313	0.232	0.130	0.073	0.098
Percent contribution	1	16	0	0	0	3
to uv in a quadrant	2	79	82	65	73	25
by quadrant	3	62	76	42	0	32
	4	12	0	0	0	2
Percent contribution	1	4	0	0	0	−1
to uv	2	79	83	65	73	25
by quadrant	3	−23	−28	−16	0	12
	4	7	0	0	0	1
$\langle u\rangle/u'$		−0.756	1.38	1.75	−1.59	−0.980
$\langle v\rangle/v'$		0.300	0.356	0.561	1.84	0.188
$\langle uv\rangle/uv$		1.87	2.33	3.78	10.02	1.36

TABLE 3. Comparison of conditionally sampled quantities during an ejection to those detected by various probe detection algorithms at $y^+ = 15$

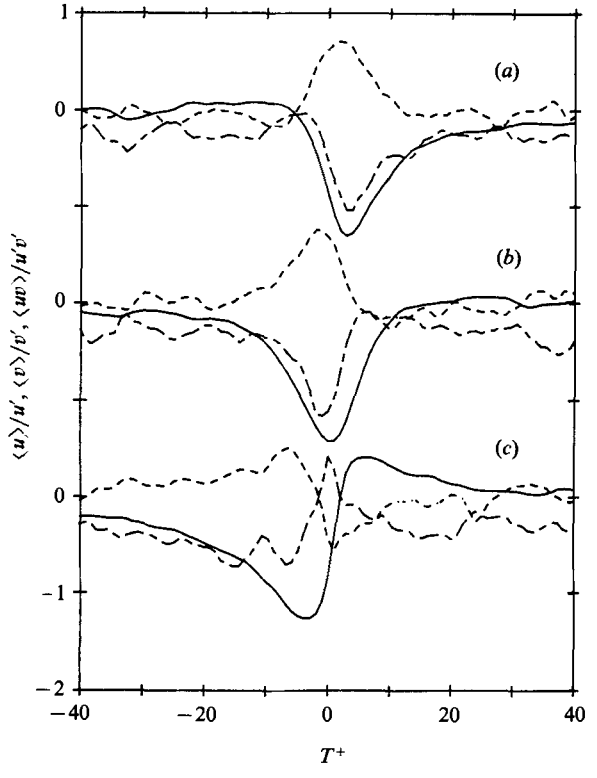

FIGURE 11. Conditionally averaged velocity signals using the modified *u* level technique centred on (*a*) leading edge, (*b*) middle, (*c*) trailing edge. ·, $\langle u\rangle$; - · $\langle v\rangle$; - - -, $\langle uv\rangle$.

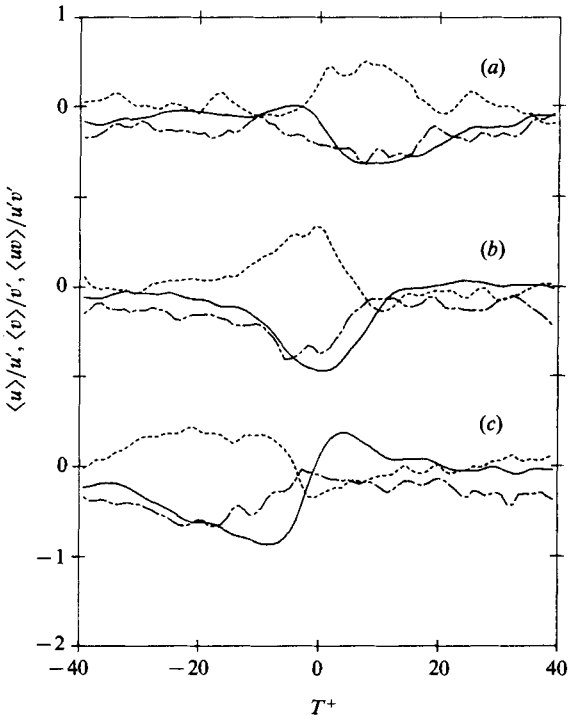

FIGURE 12. Conditionally averaged velocity signals using flow visualization (after Bogard 1982) centred on (*a*) leading edge, (*b*) middle, (*c*) trailing edge. ——, $\langle u\rangle$; – – –, $\langle v\rangle$; —·—, $\langle uv\rangle$.

of this detection is less than 25 % of the duration of the average ejection event. The u-level and VITA techniques also detect some portion of the ejection event, however, from this table it is unclear upon what portion of the event these techniques are focusing. The rather poor correspondence of VITA with the quantities obtained from flow visualization is not surprising since the technique was only detecting about half of the visual ejections when $N_D = 164$.

Average signal characteristics using the modified u-level technique are shown in figure 11. In the figure and throughout the rest of the text, a conditionally averaged quantity is shown by that quantity located within the operator $\langle\ \rangle$. Characteristics using flow visualization to detect ejections are shown in figure 12. A comparison of figures 11 and 12 shows that steeper gradients in $\langle u\rangle$ and $\langle uv\rangle$ are obtained at the leading and trailing edge of the events using the modified u-level, than were obtained from flow visualization. This was not unexpected since the visual data had a broader distribution in the duration of events than did the probe-detection data and thus would yield increased phase scrambling at the extremities of the event. This is also shown by the broader peak in the $\langle u\rangle$ signal centred on the middle of the detection of the ejection. However, the average signal patterns obtained using the modified u-level technique are reasonable estimates of those obtained using flow visualization. Because of this and the good comparison with the flow visualization in the ensemble quantities presented in table 3, as well as the fact that the modified u-level technique had the highest probability for detecting an ejection, $P(\mathrm{E})$, when $N_D \approx N_E$, the modified u-level technique was used to obtain ejection and burst characteristics at $y^+ = 30$.

Re_h		8700	17800
$\bar{T}_E$(s)		0.876	0.0301
$\bar{T}_{DE}$(s)		0.208	0.079
T^+_{DE}		13.8	12.4
Intermittency		0.237	0.262
Percentage contribution	1	0	0
to $\overline{uv}$ in a	2	87	84
quadrant by	3	67	66
quadrant	4	0	0
Percentage contribution	1	0	0
to $\overline{uv}$	2	76	83
by quadrant	3	−16	−25
	4	0	0
$\langle u\rangle/u'$		−1.362	−1.224
$\langle v\rangle/v'$		0.546	0.399
$\langle uv\rangle/\overline{uv}$		2.56	2.30

TABLE 4. Conditionally sampled quantities at $y^+ = 30$ during an ejection detection using the modified u-level technique with $L = |\bar{u}_2|/u'$

4.1. *Average signal levels associated with an ejection*

Since there is a continuous variation of the number of probe detections with threshold level, it was necessary to determine the appropriate threshold level for the detection technique prior to obtaining the conditional averages. At $y^+ = 15$ and $Re_h = 8700$ the threshold level was $L = 1$ which was determined from both the probability profile and a prior knowledge of the average time between ejections. Since the leading edge of the visual ejection was associated with a strong $-u$ component and a second quadrant uv product, the threshold level of the detector function should be associated with the same level of second quadrant u. At $y^+ = 15$, the average value of u in the second quadrant was such that

$$\frac{|\bar{u}_2|}{u'} = 1.004. \tag{29}$$

Thus the threshold level chosen to obtain ejection and burst characteristics was

$$L = \frac{|\bar{u}_2|}{u'}. \tag{30}$$

It is interesting to note that for all of the data used in the present study, $8700 \leqslant Re_h \leqslant 17800$, this threshold level was nearly equal to one which is effectively the value of L that was used in the prior probe detections and that yielded $P(\mathrm{E}) \approx P(\mathrm{D})$.

Table 4 gives the same conditionally sampled quantities as those given in table 3 when ejection detections were made using the modified u-level technique, with the threshold level determined by (30), at the highest and lowest Reynolds numbers used in the present study. At $Re_h = 8700$ and $y^+ = 30$ a greater number of probe detections are made than at $y^+ = 15$ resulting in a lower value of $\bar{T}_E$; however, the duration of the event decreases correspondingly resulting in nearly the same value of intermittency, about 0.235. Thus, the uv contribution due to a randomly occurring event would be about 23.5 %. The occurrence of higher levels in quadrants 2 and 3 indicate that the ejection event is correlated with second and third quadrant turbulent

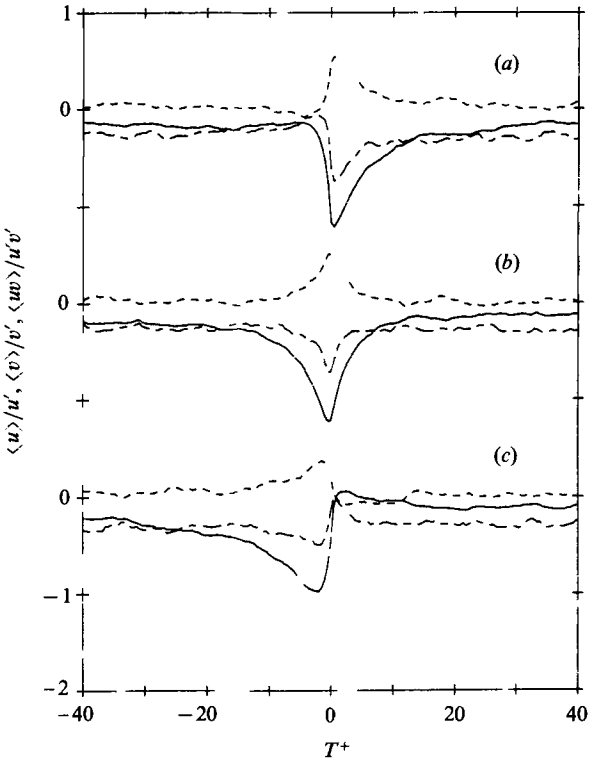

FIGURE 13. Conditionally averaged velocity signals for the water flow centred on (*a*) leading edge, (*b*) middle, (*c*) trailing edge. – , u ; , $\langle v\rangle$; , $\langle uv\rangle$; $Re_h = 17800$.

momentum transport. Also at $y^+ = 30$, although larger portions of second and third quadrant uv occur during an ejection event, the second quadrant uv contribution to $\overline{uv}$ during an ejection is about the same as at $y^+ = 15$ while there is a marked decrease in quadrant 3 contribution to uv at $y^+ = 30$. The average streamwise velocity defect, relative to u', and the average uv, relative to $\overline{uv}$ are about the same at $y^+ = 30$ as $y^+ = 15$ while $\langle v\rangle/v'$ is seen to increase at $y^+ = 30$ indicating much stronger fluid movement normal to the wall at this location than at $y^+ = 15$.

As Reynolds number increases from $Re_h = 8700$ to $Re_h = 17800$, there is a slight increase in the intermittency of ejections, a slight increase in the negative contribution of quadrant 3 uv to $\overline{uv}$ and small decreases in $\langle u\rangle$, $\langle v\rangle$ and $\langle uv\rangle$ relative to u', v' and $\overline{uv}$, respectively. However, the changes that take place are rather small in all cases which indicates that there is very little change in the relationship between the flow structure and the mean flow quantities in this Reynolds number range.

Figure 13 shows conditionally averaged velocity traces for the flow at $Re_h = 17800$ centred on the leading edge, middle and trailing edge of an ejection detection. Care must be taken when drawing conclusions from these conditional averages since phase scrambling will occur when $T^+ \neq 0$. In the present study, times less than $\frac{1}{2}$ the average duration of the event away from the centre of the conditional averages ($T^+ \approx \pm 6$) were considered relatively good representations of individual signals. At the leading edge of the event, sharp negative gradients in $\langle u\rangle$ and $\langle uv\rangle$ occur while a sharp positive gradient of the normal component of velocity occurs. The converse is true at the trailing edge of the event. The magnitude of the gradient of the streamwise

Re_h		8700	17800
$\bar{T}_B$(s)		2.00	0.0632
Average number of ejections/burst		2.28	2.10
$\bar{T}_{DB}$(s)		0.784	0.0235
T^+_{DB}		52.6	36.8
Intermittency		0.392	0.372
Percentage contribution	1	14	37
to uv in a	2	93	89
quadrant by	3	82	76
quadrant	4	13	7
Percentage contribution	1	−2	−2
to uv	2	81	88
by quadrant	3	-19	29
	4	7	5
$\langle u \rangle / u'$		−0.786	−0.865
$\langle u \rangle\ v'$		0.288	0.244
$\langle uv \rangle / uv$		1.664	1.680

TABLE 5. Conditionally sampled quantities at $y^+ = 30$ during a burst detection using the modified u-level technique with $L = |\bar{u}_2|,\ u'$

component of velocity is slightly greater near the trailing edge of the event than at the leading edge. The opposite is true of the $\langle v \rangle$ and $\langle uv \rangle$ signals. Similar results were noted by Bogard (1982) at $y^+ = 15$ for visually detected ejections. Upon comparing the conditional averages at $y^+ = 15$ and $Re_h = 8700$ (figure 11) with those at $y^+ = 30$ and $Re_h = 17800$ (figure 13), it is apparent that the temporal gradients in $\langle u \rangle$, $\langle v \rangle$, and $\langle uv \rangle$ associated with an ejection at both the leading edge and trailing edge of the event increases as Reynolds number increases when time is normalized with inner variables. A similar effect is seen when time is normalized with outer variables.

4.2. *Average signal levels associated with a burst*

The conditionally sampled quantities obtained during a burst detection at $y^+ = 30$ for $Re_h = 8700$ and 17800 are given in table 5. Similar trends are obtained for the burst structure as were obtained for the ejection structure. This again indicates that the relationship of the burst structure to the time-averaged flow properties does not change much with increasing Reynolds number.

Figures 14 and 15 show conditional velocity traces centred on the leading and trailing edge of a burst respectively. Comparing these figures with figure 13(*a* and *c*) shows that the $\langle u \rangle$, $\langle v \rangle$ and $\langle uv \rangle$ signals for the burst event are similar to those for the ejection event. As before, a large quadrant 2 peak in $\langle uv \rangle$ occurs just after the leading edge of the burst while there is almost no quadrant 2 peak in $\langle uv \rangle$ associated with the trailing edge of the burst.

The major difference between the conditionally averaged signals for the burst and ejection are that $\langle u \rangle$ is higher than $\bar{u}$ and $\langle v \rangle$ is less than zero both prior to and after the burst event. These 'sweep' type characteristics are not evident in the $\langle u \rangle$ and $\langle v \rangle$ signals averaged over all ejections. Bogard (1982) also noted these trends at $y^+ = 15$ using flow visualization to detect the ejection events. These results support the view that sweep-type motions correlate better with the burst event than the ejection event and that the sweep structure can be found at either extreme of a burst.

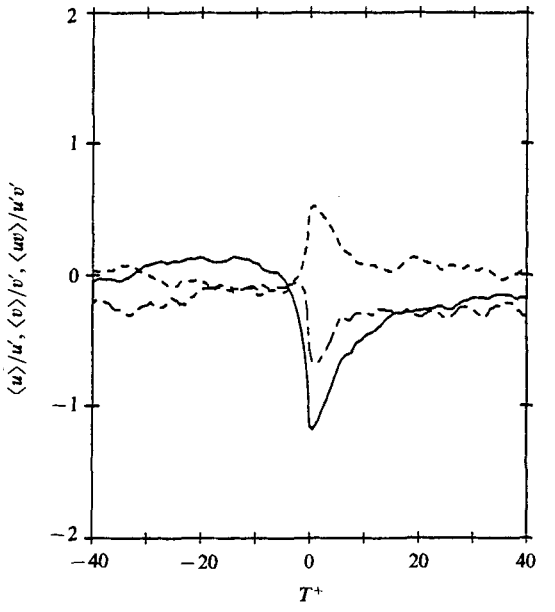

FIGURE 14. Conditionally averaged velocity signals for the water flow centred on the leading edge of the first ejection in a burst. ——, $\langle u\rangle$; – – –, $\langle v\rangle$; — · — $\langle uv\rangle$; $Re_h = 17800$.

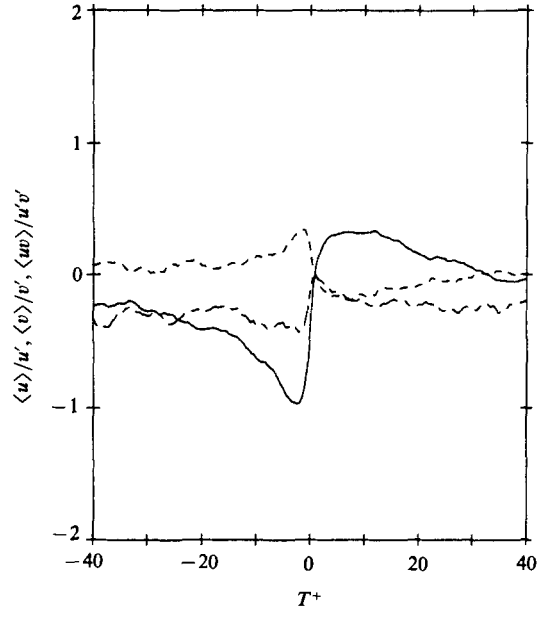

FIGURE 15. Conditionally averaged velocity signals for the water flow centred on the trailing edge of the last ejection in a burst. ——, $\langle u\rangle$; – – –, $\langle v\rangle$; — – — –, $\langle uv\rangle$; $Re_h = 17800$.

This view also is consistent with the fact that a single burst may contain several ejections.

Since the probe techniques presented were devised to detect the burst event and not the sweep event, care must be taken in attempting to draw conclusions about the sweep event from figures 14 and 15. However, the magnitude of the positive $\langle u\rangle$

and negative $\langle v \rangle$ levels following the burst are larger than those seen leading the burst. There is also a trend that the $\langle uv \rangle$ signal following the burst is consistently negative and is in fact a quadrant 4 uv product (positive u, negative v) whereas the $\langle uv \rangle$ leading the burst is smaller. These trends indicate that the sweep event following the burst has more in-rush type quality and makes a larger contribution to positive uv than the event leading the burst.

5. Conclusions

The burst-detection techniques developed in the present study as well as the $uv|_2$ technique with the grouping parameter determined using the exponential distribution all yield accurate estimates for the average time between bursts. In terms of accuracy, the uv quadrant 2 technique gave the most accurate estimate of the average time between bursts; however, the technique did not detect the entire burst or ejection event. Overall, the modified u-level technique did yield a good estimate of the average time between bursts when used with the appropriate value of the grouping parameter as well as yielding representative conditional averages when the threshold level was set using (30). The VITA technique with the grouping parameter also yielded an accurate estimate of the average time between bursts even when only small data sets were available. However, the present results were obtained with significantly lower threshold values than are commonly used with this technique. Critical comparison of the three alternatives (inner, mixed, outer) for scaling the average time between bursts showed that outer scaling does not work. Inner scaling appears to be more appropriate than mixed scaling. Results at higher Reynolds numbers are needed to remove any doubt about the dimensionless value of $\bar{T}_B$.

This research was supported by a David Ross Grant from Purdue University and the Office of Naval Research, Contract number N00014-83K-183, NR062-754.

REFERENCES

ALFREDSSON, P. H. & JOHANSSON, A. V. 1984 Time scales for turbulent channel flows. *Phys. Fluids* **27**, 1974.

BLACKWELDER, R. F. & HARITONIDIS, J. H. 1983 Scaling of the bursting frequency in turbulent boundary layers. *J. Fluid Mech.* **132**, 87.

BLACKWELDER, R. F. & KAPLAN, R. E. 1976 On the structure of the turbulent boundary layer. *J. Fluid Mech.* **76**, 89.

BOGARD, D. G. 1982 Investigation of burst structures in turbulent channel flows through simultaneous flow visualization and velocity measurements. Ph.D. thesis, Purdue University.

BOGARD, D. G. & TIEDERMAN, W. G. 1983 Investigation of flow visualization techniques for detecting turbulent bursts. In *Symposium on Turbulence, 1981* (ed. X. B. Reed, G. K. Patterson & J. L. Zakin), p. 289. University of Missouri, Rolla.

BOGARD, D. G. & TIEDERMAN, W. G. 1986 Burst detection with single point velocity measurements. *J. Fluid Mech.* **162**, 389.

CORINO, E. R. & BRODKEY, R. S. 1969 A visual study of turbulent shear flow. *J. Fluid Mech.* **37**, 1.

DEAN, R. B. 1978 Reynolds number dependence of skin friction and other bulk flow variables in two-dimensional rectangular duct flows. *Trans. ASME I: J. Fluids Engng* **100**, 215.

JOHANSSON, A. V. & ALFREDSSON, P. H. 1982 On the structure of turbulent channel flow. *J. Fluid Mech.* **122**, 295.

KIM, H. T., KLINE, S. J. & REYNOLDS, W. C. 1971 The production of turbulence near a smooth wall in a turbulent boundary layer. *J. Fluid Mech.* **50**, 133.

LU, S. & WILLMARTH, W. W. 1973 Measurements of the structure of Reynolds stress in a turbulent boundary layer. *J. Fluid Mech.* **60**, 481.

LUCHIK, T. S. 1985 The effect of drag-reducing additives on the turbulent structure in channel flows. Ph.D. thesis, Purdue University.

LUCHIK, T. S. & TIEDERMAN, W. G. 1984 Bursting rates in channel flows and drag-reducing channel flows. In *Symposium on Turbulence, 1983* (ed. X. B. Reed, G. K. Patterson & J. L. Zakin), p. 15. University of Missouri, Rolla.

OFFEN, G. R. & KLINE, S. J. 1975 A comparison and analysis of detection methods for the measurement of production in a boundary layer. In *Proc. 3rd Biennial Symp. on Turbulence in Liquids* (ed. G. K. Patterson & J. L. Zakin), p. 289. University of Missouri, Rolla.

ROBINSON, S. K. 1982 An experimental search for near-wall boundary conditions for large eddy simulation. *AIAA Paper* 82-0963, St Louis, Missouri.

TIEDERMAN, W. G., LUCHIK, T. S. & BOGARD, D. G. 1985 Wall-layer structure and drag reduction. *J. Fluid Mech.* **156**, 419.

WILLMARTH, W. W. & SHARMA, L. K. 1984 Study of turbulent structure with hot wires smaller than the viscous length. *J. Fluid Mech.* **142**, 121.